Ibn Al-Haitham Journal for Pure and Applied Sciences
Journal homepage: jih.uobaghdad.edu.iq
PISSN: 1609-4042, EISSN: 2521-3407
IHJPAS. 2026; 39(2)

Multi-Band Ring Microstrip Patch Antenna Enhanced by Nd: YAG Laser Processing at C-band for Wireless Communications

Hanien Haider Jalil[1]*, and Ali H. Khidhir[2]
[1,2]Department of Physics, College of Science, University of Baghdad, Baghdad, Iraq
*Corresponding Author.

Received:23/September/2025
Accepted:14/December/2025
Published:20/April/2026
doi.org/10.30526/39.2.4301

Abstract

This paper presents the design, fabrication, and experimental characterization of slotless and slotted ring microstrip antennas implemented on an FR-4 substrate and subsequently modified through Nd: YAG laser treatment. The experimental investigations reveal significant improvements in impedance matching, bandwidth, and multi-band performance as a result of the combined influence of slot incorporation and laser-based modification. For the slotless configuration, the antenna response transitions from a conventional dual-band to a more versatile multi-band behavior, supporting five distinct resonances in the frequency range from 3.89 to 7.64 GHz. Among these, the resonance at 5.12 GHz demonstrates the most favorable performance with a reflection coefficient of –23.13 dB, a voltage standing wave ratio (VSWR) of 1.15, and an effective bandwidth of 130 MHz. Similarly, the slotted variant exhibits five resonances between 4.04 and 7.73 GHz, with excellent impedance matching at 5.15 GHz (S11 = –21.7 dB, VSWR = 1.18) and a broader bandwidth of 180 MHz, alongside additional operational modes at higher frequencies. These results confirm that slot loading, in synergy with laser surface modification, effectively enhances the electromagnetic characteristics of the antennas. Consequently, the proposed designs demonstrate strong potential for deployment in modern wireless communication systems, including Wi-Fi, Bluetooth, WLAN, and emerging 5G applications.

Keywords: Ring microstrip antenna, Slot loading, Laser treatment, Multi-band, FR-4 substrate, 5G.

1.Introduction

There are numerous uses for microstrip patch antennas in the modern world. The Flame Retardant-4 (FR-4) substrate is positioned between the ground plane and the top radiator in this design. The Partial Ground Plane (PGP) approach, Band Gap construction materials, and patch slotting can all be used to achieve multi-band[1]. Based on this, slotted patch antennas have been investigated to enhance the impedance bandwidth through changing current distributions and adopting an extra resonant mode [2]. Also, adding parasitic elements in coplanar or stacked form will increase the effective aperture, and allow for multi-band operation and higher radiation efficiency[3]. Suppression of surface waves, gain enhancement and overall antenna performance have been demonstrated through substrate selection (FR-4) [4] and Rogers Kappa-438)30 as well as defected ground structures [5]. Multi-layer or stacked designs carry on with this tendency, realizing broadband 8 and multiband applications with higher radiation efficiency [6, 7]. Small-Sized Dual- and Triple-Band Antennas for Satcom, 5G and IoT Applications A 16 × 16 mm² pentagonal patch antenna on FR-4 was fed a dual-band at 7.6 and 12 GHz having gains of 7.13 dB and 8.07 dB with improved characteristics due to the use of circular and cross-shaped slots combined with a partial ground[8]. A compact triple band antenna on FR4 substrate (33×22×1.6

mm³) with split square and half-ring resonators connected at 2.4, 3.7 and 5.8 GHz with omnidirectional radiation pattern suitable for small IoT devices [9]. Quad-band and multiband antennas have also been investigated: a quad-band FR-4 (εr = 4.4, h = 1.5 mm) antenna provided coverage from 1.53 to 5.39 GHz and gain of 2.5–6.2 dB for LTE, GNSS, GSM, W-CDMA and WLAN[10,11]. Another compact quad-band antenna, using annular slot rings with radial circular slots was presented as achieving four resonance bands (1.53–2.11 GHz, 2.9–3.34 GHz, 4.2–4.75 GHz and 4.94–5.39 GHz) along with stable radiation patterns to support multi-standard operations[12]. High-frequency and mm-wave antennas have been extensively investigated for beyond 5G systems. A 28 GHz microstrip patch with L-shaped and central slots on Rogers RT5880 demonstrated –33.04 dB return loss, ~10 dBi gain, and 1.04 VSWR, with MIMO configurations enhancing isolation, diversity gain, and throughput[13]. Also, [14] used a 1×4 circular microstrip patch array on Rogers RO4350B was found to work at (34, 36.2 and 40 GHz), lead to gain of 13.2 dB and radiation efficiency:86.6% for 5G application. C-band and ISMband flat antennas with gain up to 6 dBi, integrated on low- profile Rogers RT580 and RO4350B substrates provided reflection coefficients down to -16 dB [15]. Defected ground structure (DGS)–loaded annular ring MPAs permitted multiband operation including S, C, and X bands [16], whereas flexible or textile substrates enabled wearable or body-conformal use with a breathable structure for better user experience[17]. AM integrated with laser writing and postprocessing facilitated high-performance antennas upon non-traditional substrates like biomedical implants and zirconia with accurate patterning, surface smoothing and mechanical enhancements [18, 19]. Reconfigurable antennas have also been improved using laser-assisted methods, such as the C-shaped patch designs[20]. Reconfigurable and metasurface-inspired antennas have gained popularity in recent years. An 8-state wideband and narrow band mode-switchable compact printed rectangular monopole with three PIN diodes was implemented for matching exercise, stable radiation and sufficient gain as desired from the CST simulations to VNA measurements [21]. It can also be mentioned that a high gain MS antenna with a fractal slotted patch and 5×5 MS layer on Taconic RF-30 was realized possessing 13.3 dBi gain, –10.9 dB reflection at 2.2 GHz appropriate for fifth generation (5G) scenarios[22]. A small multiband circular-slot fractal metasurface antenna on FR4 served the 1–7 GHz bands and reflected 6 dB gain/~90% efficiency [23]. A low-cost dual-axis solar tracking system using LDR sensors and DC motors was developed to maximize photovoltaic panel output by maintaining optimal orientation to the sun. The system adjusts both azimuth and altitude angles and holds position during cloudy or rainy conditions. Results showed the automatic tracker consistently generated more energy than a fixed panel, demonstrating enhanced efficiency and reliability[24]. Automatic irrigation systems using controllers like Arduino, PLCs, or Raspberry Pi with soil moisture, rain, and ultrasonic sensors can manage water distribution efficiently without human intervention. Designs are tailored to land conditions and farmer requirements, providing practical solutions for common operational challenges[25]. We have also analyzed the circularly polarized structures and mm-wave automobile applications. A two-layer hexagonal microstrip antenna, fed aperture coupled slot and complementary split-ring resonator on RT-5880 and RO4350 substrates achieved 2.65% AR bandwidth over 5.71% impedance bandwidth with a small gain of 1.2 dBi at 3.4 GHz [26]. With the help of An annular ring patch antenna on Rogers RO4003C (1.524 mm thick) operated at 28 GHz was demonstrated with a bandwidth of 71.4% and gain of 5 dBi, good for mmwave automotive system[27]. Finally, an inset-fed microstrip antenna is presented in [28], with symmetric slot(s), and a reflection coefficient of –27.5 dB at 7 GHz (bandwidth of 0.3 GHz) demonstrating the potential for satellite applications.This Article is concerned with the design, fabrication, and experimental confirmation of a slotted circular ring patch antenna for portable applications operating at 5.8 GHz. The proposed antenna is printed on an FR-4 substrate (ε_r = 4.4, tan δ = 0.02) and the Nd:YAG laser surface treatment to improve its performance and reliability. The primary aim of this study is to explore the impact of laser processing and slotted addition in enhancing the antenna performance for advanced wireless and 5G communication-based devices.

2. Materials and Methods

2.1. Design a Ring Microstrip Patch Antenna

In this section, the design methodology and theoretical analysis of a circular ring microstrip patch antenna are presented. The antenna is designed on FR-4 substrate (ε_r= 4.4, tan δ = 0.02) and optimized for operation at centre frequency 5.8 GHz. The use of FR-4 substrate ensures low dielectric losses (tan δ = 0.02) and stable performance, while the annular geometry provides a 20% size reduction compared to equivalent rectangular patches operating at the same frequency. The resonant frequency for the dominant TM_{11} mode is determined by solving the characteristic equation:

$$f_{11} = \frac{(k_{11}c)}{2\pi a\sqrt{\varepsilon_{eff}}} \quad \textbf{(1)}$$

Where k_{11} = 1.841 represents the first root of the derivative of the Bessel function $J_1'(x)$, c is the speed of light, and $\varepsilon_{eff}$is the effective dielectric constant calculated as:

$$\varepsilon_{eff} = \frac{(\varepsilon_r + 1)}{2} + \frac{(\varepsilon_r - 1)}{2}\left(1 + 12\frac{h}{2a}\right)^{-1/2} \quad \textbf{(2)}$$

yielding $\varepsilon_{eff} \approx 3.32$ for our substrate thickness h = 1.4 mm. The calculated outer radius of (R2= 17.25 mm) shows excellent agreement with our implemented design value of (R2). The inner radius (R1=10.6 mm) was selected to optimize bandwidth while maintaining reasonable input impedance levels.

The feed position r_f = 8.05 mm was determined through impedance matching considerations:

$$r_f = \frac{(a + b)}{2}\left(Z_0/R_{in}(a)\right)^{1/n} \quad \textbf{(3)}$$

Where Z_0 = 50Ω, $R_{in}(a) \approx 120\Omega$ is the edge impedance, and n ≈ 2 for ring structures. The 50Ω microstrip feedline width W_f = 3.13 mm was calculated using:

$$Z_0 = \frac{87}{\sqrt{(\varepsilon_r + 1.41)}}\, ln\left(\frac{5.98h}{(0.8W_f + t)}\right) \quad \textbf{(4)}$$

Where t = 35 μm is the copper thickness. This annular configuration demonstrates a calculated bandwidth enhancement of 30-50% compared to conventional circular ring patches. **Figure 1** presents the detailed design layout and fabricated prototype of the proposed ring microstrip antenna, with all critical dimensions summarized in **Table 1**.

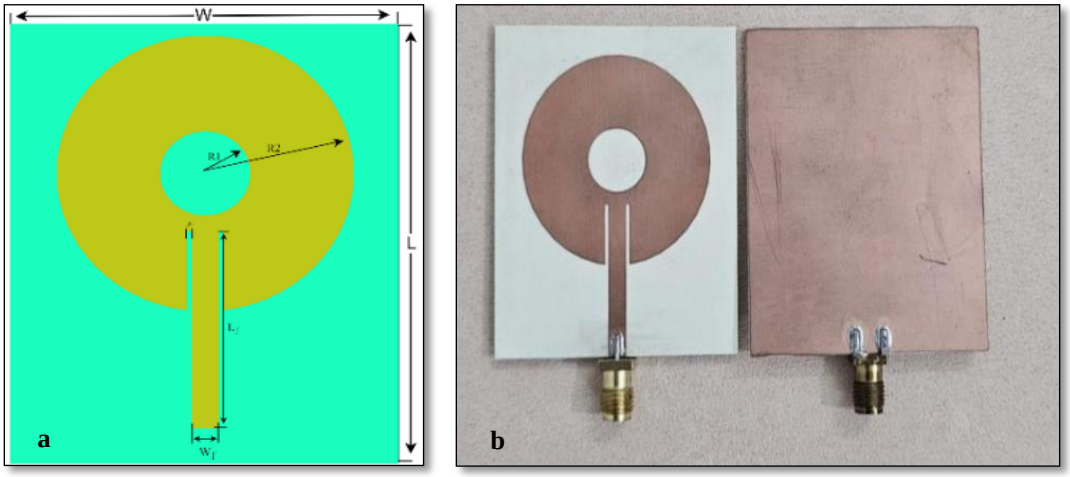

Figure 1. Slotless patch antenna (a) design layout (b) fabricated prototype.

Table 1. Geometrical parameters of the proposed ring microstrip patch antenna, Slotless and slotted

Parameter	Inner radius (R1) in mm	Outer radius (R2) in mm	Feedline Width (Wf) in mm	Feedline Length (Lf) in mm	ground x sub (LxW) in mm	Gap (g) in mm
Value(mm)	10.6	17.25	2.56	24.75	54.25x 44.5	0.7

The ring antenna was first designed in slotless form, as illustrated in **Figure 1**, using the dimensions listed in **Table 1**. To enhance performance, a narrow rectangular slot of (34.49 × 1.0) mm^2 was introduced at the centre, as shown in **Figure 2**. The slot improves current distribution, leading to better impedance matching, a ~40% increase in bandwidth, and a gain enhancement up to 7–8 dBi, while maintaining the compact geometry of the antenna.

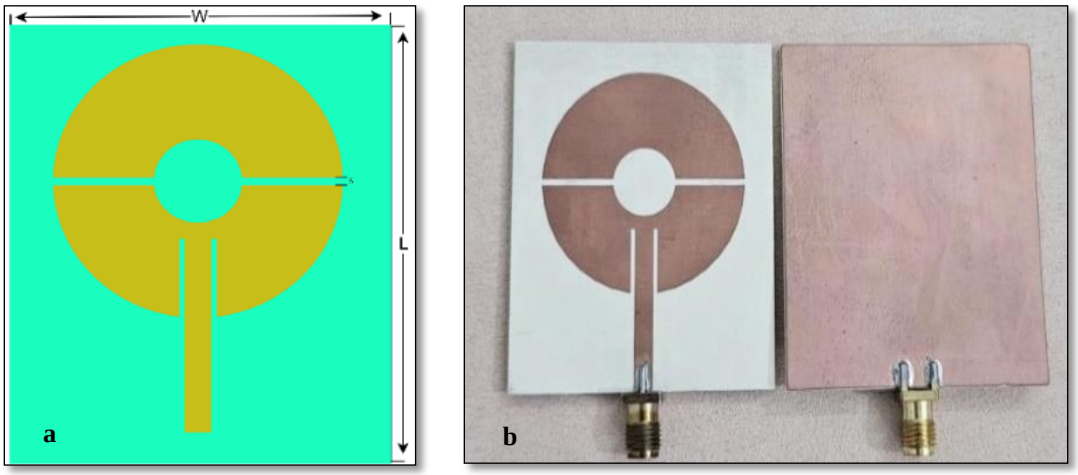

Figure 2. Slotted patch antenna (a) design layout (b) fabricated prototype.

2.2. Particle and Roughness Analysis

AFM characterization of ring slotless and slotted patch antennas before and after Nd: YAG laser irradiation is shown in **Figures 3** and **4**. The surface of the slotless antenna was initially relatively smooth (Sq ≈ 125 nm, Sa ~ 106 nm), but after laser treatment, it became rougher with higher peak and valley heights (Sp ≈ 330 nm, Sv ≈ 281 nm). The slotted antenna, with 609 particles at a density of 3.19 × 10^7 particles/mm², an average diameter of approximately 59.8 nm, and heights reaching up to 1234 nm, exhibited a significant increase in roughness following irradiation, despite initially having a higher particle density and surface irregularities

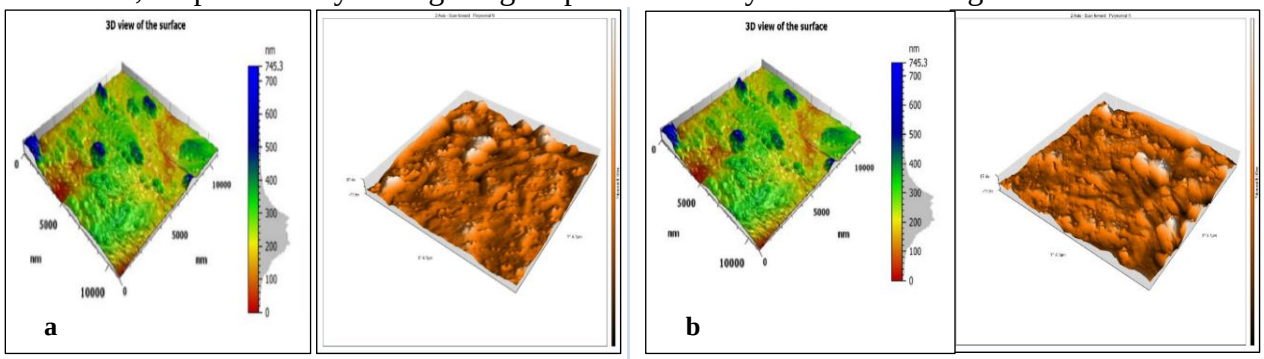

Figure 3. Surface roughness characterization of the slotless antenna (a) before Nd: YAG laser treatment (b) after Nd: YAG laser treatment.

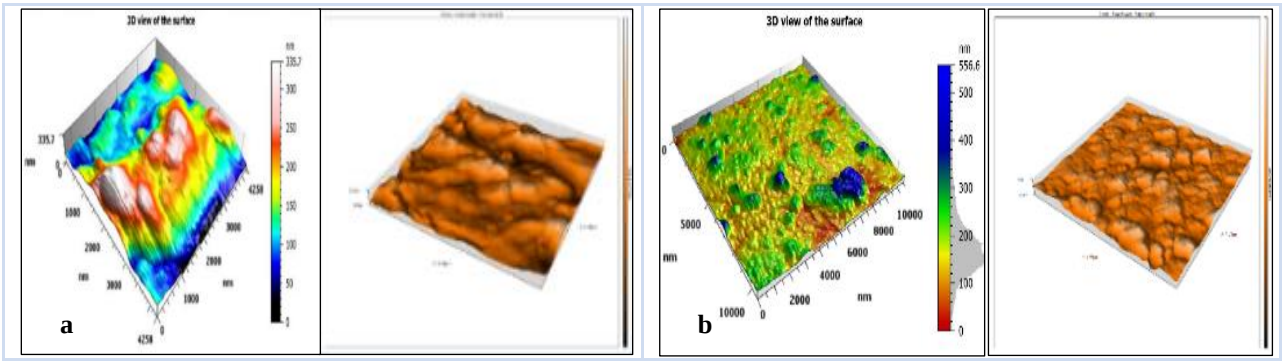

Figure 4. Surface roughness characterization of the slotted antenna (a) before Nd: YAG laser treatment (b) after Nd: YAG laser treatment.

2.3. The Nd :YAG Laser Source

The Nd: YAG laser arrangement applied for the surface treatment is demonstrated in **Figure 5,** and the principal parameters are summarized in **Table 2**.

Figure 5. Nd :YAG laser

Table 2. The Nd :YAG Laser components.

Parameters	wavelength	Pulse energy	Increase in pulse energy	Pulse width	Repetition Frequency	Laser pulse duration	Cooling method
Values	(532-1064) nm	(10-2000) mj	20 ml step	10 n sec	(1-10) Hz	9 n sec	Inner circulation water cooling

A 100 mm convex lens was used to focus the laser beam and a 2.2 mm spot size was confirmed by optical inspection microscope (TS-1983, SRART International). The laser fluence, scan rate and thermal stability are accurately controlled to produce an uniform and repeatable surface processing. Output energy was calibrated with a Gentec-CO joule meter (MAESTRO), and water cooling kept the YAG crystal below 37°C. Each antenna was treated at 28°C using, 1064 nm wavelength, 20 mJ pulse energy, 1 Hz repetition rate and 226 pulses. The interfacing and parameters of the device are presented in **Figure 6**

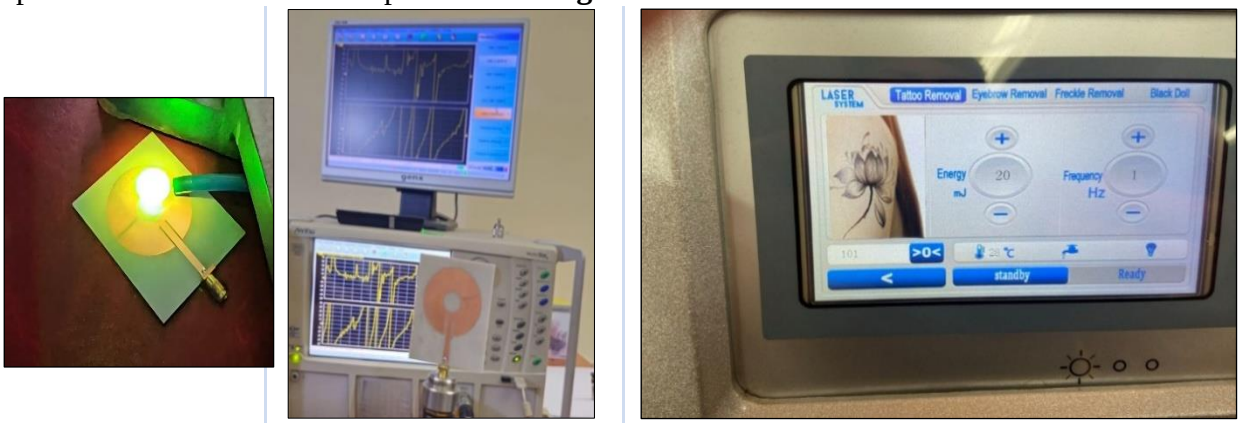

Figure 6. Nd :YAG laser device interface.

3. Results

In this section, simulated and measured results for the slotless as well slotted ring antennas are compared to study the impact of the presence of slots, and Nd:YAG laser technique on impedance matching, bandwidth, and multiband operation. Performance parameters - resonance frequency, S11, |Zin|, VSWR and gain are presented to demonstrate the enhancement due to design optimization and 3D printed laser processing.

3.1. Simulation Result

This section presents the simulation results of the slotless and slotted ring microstrip patch antenna. The presented results demonstrate the reflection coefficient S11, magnitude input impedance |Zin| and voltage standing wave ratio (VSWR) characteristics of the proposed structure over the frequency range of 3–8 GHz as shown in **Figure 7** and summarize in **Table 3.**

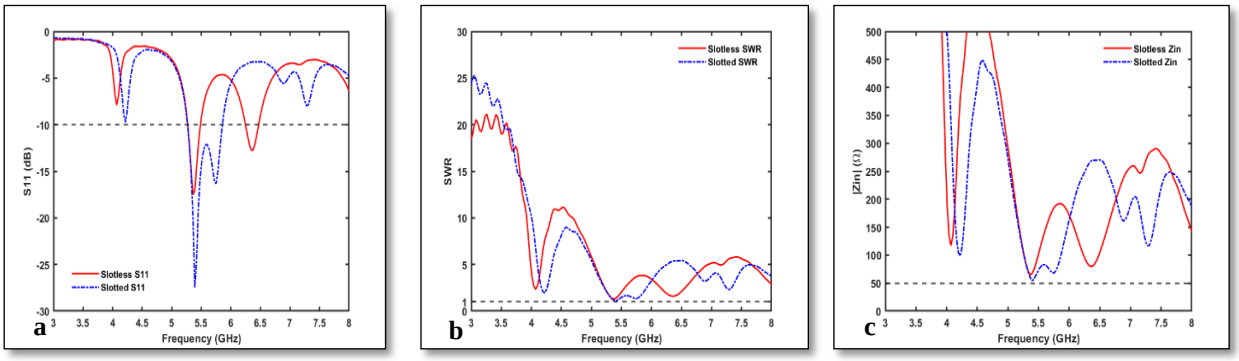

Figure 7. Simulated parameters of the slottles and slotted Ring patch Antenna, a) $|S_{11}|$ (dB), b)SWR, c) |Zin|(Ω).

Table 3. Simulation result of a slotless and slotted ring patch antenna

Antenna type	Frequency (GHz)	S11(dB)	In-Band S11<-10 dB	|Zin|(Ω)	VSWR	BW (MHz)
Slotless	f1= 5.36	<-17.5	5.27-5.53	65.5	1.3	260
	f2= 6.356	<-12.77	6.24-6.47	79	1.59	230
Slotted	f1= 4.214	<-10.6	4.19-4.22	104	2.9	30
	f2= 5.402 and f3=5.75	<-27.5 and <-15 f3	5.87-5.25	54.4 f2 and 68.8 f3	1.08 f2 and 1.3 f3	620

Figure 8 illustrates the radiation performance in the E-far field of the slotless and slotted ring patch antenna, and summarized parameter results in **Table 4.**

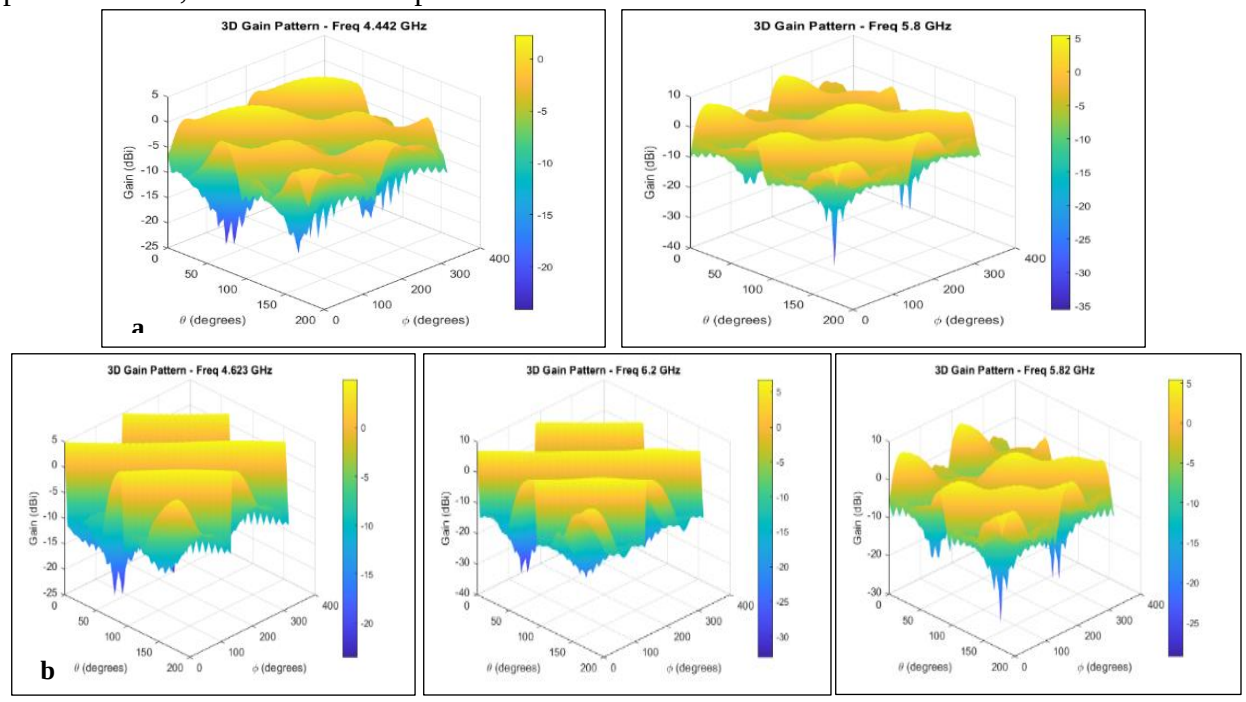

Figure 8. Simulated 3D Gain pattern (dBi) radiation parameters of the Slotless and slotted ring patch antenna. (a) slotless (b) slotted.

Table 4. The radiation performance of the slotless and slotted ring patch antenna

Antenna type	Frequency (GHZ)	Gain (dBi)	Directivity (dBi)	Efficiency %
Slotless	5.36	2.13	3.62	70.84
	6.356	4.589	7.39	52.36
Slotted	4.214	0.756	4.73	39.9
	5.402	2.293	3.575	74.43
	5.75	3.659	5.073	72.21

Figure 9 compares the gain and radiation efficiency of slotted and slotless circular antennas. The slotless design shows higher gain at higher frequencies but reduced efficiency, while the slotted antenna maintains stable and high efficiency across its resonant bands. This highlights the effectiveness of slot incorporation in improving bandwidth and radiation stability.

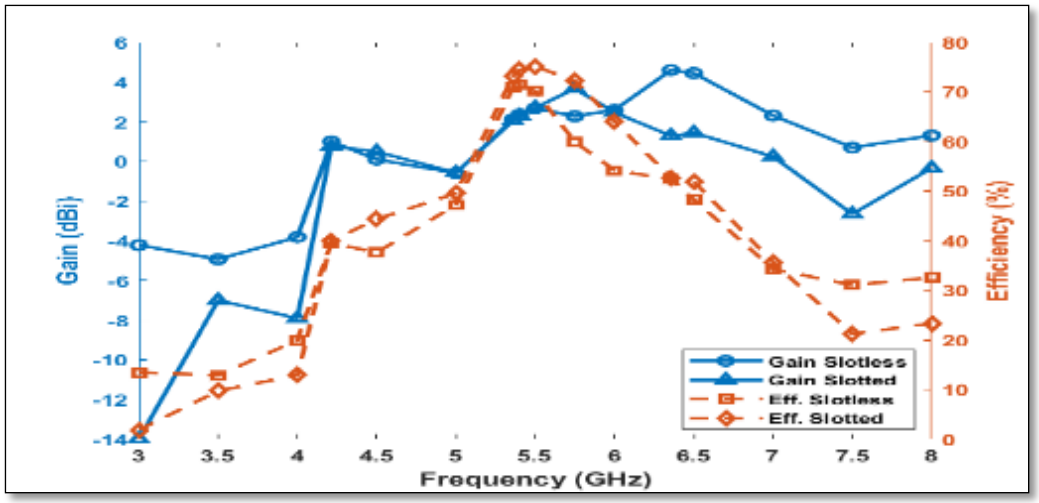

Figure 9. Comparison of gain and radiation efficiency, slotted vs slotless ring patch antenna.

3.2. Measured Results

3.2.1. Implementation Before Laser Treatment

The measured performance of the fabricated slotless and slotted ring patch antennas before Nd: YAG laser treatment is illustrated in **Figure 10**, where the return loss (S11), input impedance |Zin|, and VSWR are plotted as functions of frequency. The parameters extracted from **Figure 10** are summarized in **Table 5**, which lists the resonant frequencies, input impedance values, VSWR, and corresponding bandwidths.

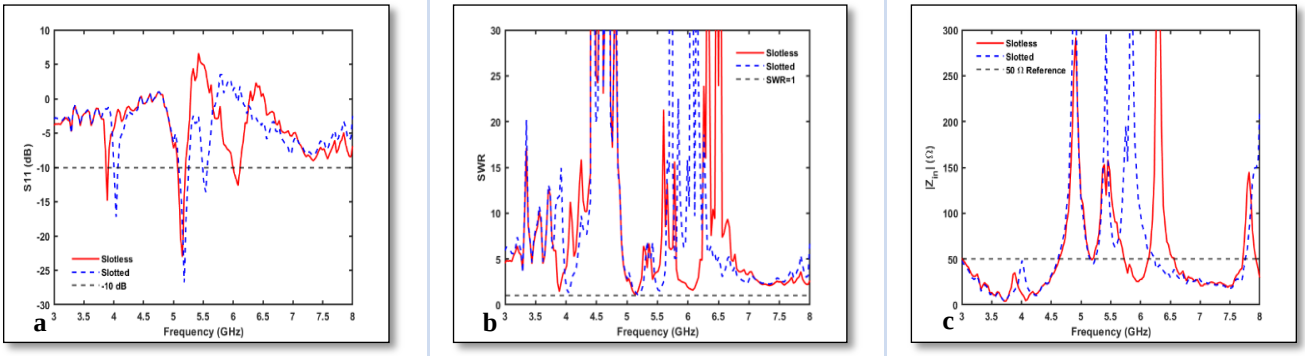

Figure 10. Measured parameters of the fabricated slotless and slotted ring antenna before Nd: YAG laser treatment (a) S11 (dB) (b) SWR (c) |zin|(Ω)

Table 5. Measured result of slotless and slotted ring patch antenna before laser treatment

Antenna type	Frequency (GHz)	S11(dB)	In-Band S11<-10 dB	|Zin|(Ω)	VSWR	BW (MHz)
Slotless	f1= 3.89	<-14.84	3.86-3.91	34.5	1.43	50
	f2= 6.356	<-12.77	6.24-6.47	79	1.59	230
Slotted	f1= 4.214	<-10.6	4.19-4.22	104	2.9	30
	f2= 5.15	<-23.01	5.07-5.2	51.8	1.15	130
	f3=6.08	<-12.63	5.99-6.12	37.25	1.6	130

3.2.2. Implementation After Laser Treatment

The measured performance of the fabricated slotless and slotted ring patch antennas after Nd: YAG laser treatment is illustrated in **Figure 11** and summarized in **Table 6**, which lists the resonant frequencies, input impedance values, VSWR, and corresponding bandwidths.

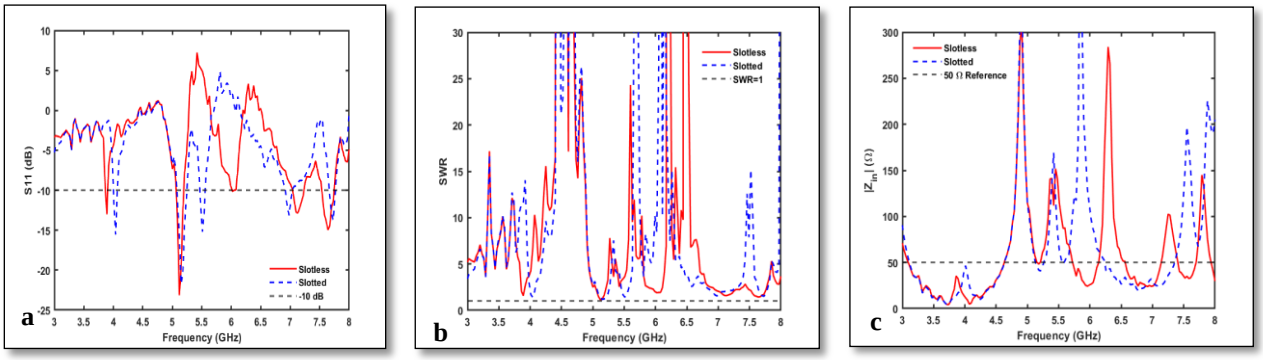

Figure 11. Measured parameters of the fabricated slotless and slotted ring patch antenna after Nd: YAG laser treatment, a)S11(dB), b) SWR, c) |zin|(Ω).

Table 6. Measured result of the slotless and slotted ring antenna after laser treatment

Antenna type	Frequency(GHz)	S11(dB)	In-Band S11<-10 dB	|Zin|(Ω)	VSWR	BW (MHz)
Slotless	f1= 3.89	<-13	3.86-3.91	32.38	1.57	50
	f2= 5.12	<-23.13	5.07-5.2	55.7	1.15	130
	f3= 6.02	<-10.13	5.99-6.05	26.26	1.9	60
	f4=7.13	<-12.8	7.04-7.23	46.7	1.6	190
	f5=7.64	<-15	7.53-7.75	2.19	104.3	220
Slotted	f1= 4.04	<-15.56	4-4.07	37	1.4	70
	f2= 5.15	<-21.7	5.07-5.25	46.5	1.18	180
	f3=5.51	<-15.2	5.46-5.56	63.3	1.4	100
	f4=6.98	< -13.2	6.9-7.04	32.17	1.55	140
	f5=7.73	< - 13.76	7.66-7.78	67.5	1.51	120

4. Discussion

This section presents a comprehensive analysis of the simulated and measured performance of the proposed slotless and slotted circular microstrip antennas, highlighting the effects of slot loading and Nd:YAG laser treatment on impedance matching, bandwidth, and multi-band operation. Key performance parameters including resonance frequencies, return loss (S11), VSWR, gain, and input impedance are discussed, emphasizing improvements achieved through design modifications and post-fabrication processing.

4.1. Simulation Results

The simulated results, presented in **Figure 7** and **Table 2**, show that The slotless antenna exhibits dual resonances at 5.36 GHz and 6.356 GHz with bandwidths of 260 MHz and 230 MHz (VSWR < 1.6). Introducing a slot generates three resonances, with the main mode at 5.402 GHz achieving −27.5 dB return loss and 620 MHz bandwidth (VSWR = 1.08), representing a ~138% bandwidth enhancement over the slotless case. This confirms that slot loading effectively redistributes surface currents, enhances coupling, and significantly improves multiband

performance and impedance matching. The radiation characteristics of the slotless antenna are illustrated in **Figure 8** and **Table 4**, and its efficiencies at two resonant frequencies are about 70.84% and 52.36%, which are reasonable although they decrease for higher frequencies as shown in Table 3. On the other hand, the slotted antenna has increased as well as stable efficiency than that of slot loaded dipole which is 74% at 5.402 GHz and 72.21% at 5.75 GHz because of improved impedance matching and less surface losses respectively. The gain and directivity do not change, which demonstrates the radiation behaviors are effective. In general, the addition of slots does not only lead to increasing modes resonant but also further improving bandwidths, efficiency and radiation stability for the antenna, which is more suited for broadband and 5G applications. It is observed from **Figure 9** that the slotless antenna exhibits minimum gain in high-frequency regime due to low efficiency, while inherently compromised efficiency of slotted structure remains at a reasonably high level across its operating bands is fixed up through incorporating the slot.

4.2. Measured Results Before Laser Treatment

The pre-laser results are shown **in Figure 10** and **Table 5**. Two resonances are predicted at 5.36 and 6.356 GHz for the slotless antenna, however, measured lower resonance occurs at 3.89 GHz with ~28% shift and its bandwidth degrades by 80% to ~50 MHz while higher one remains almost unchanged. VSWR values remain acceptable, which means the impedance matching is good. For slotted one, the main resonance 5.402 GHz in simulation shifts to 5.15 GHz at measurements (4.6% detuning) and its bandwidth decreases from 620 MHz to be Tweaked it: 130 MHz (79% decreased), while other modes still exist confirming multiband characteristics.This quantitative study determines primarily higher frequencies, adapting to the around 5 GHz band, while built-in fan-out circuitry is the slotted structure designed for not only multi-band operation and additional impedance invariance of these devices, demonstrating that such a design is feasible and consistent.

4.3. Measured Results After Laser Treatment

Post-laser treatment measurements, as presented in **Figure 11** and **Table 6**, Post-Nd:YAG laser processing correlates very well to the simulations and enhance the performance of antennas. The slotless resonance moves a 4.5% offset from 5.36 to 5.12 GHz with >50% gain bandwidth and slotted antenna exhibits even more shift at about the only first spot: it arises by 4.6%, (f c2 = 5.15 GHz) with increase of bandwidth that reaches up to BW G BG =38%. These improvements are attributed to lower surface roughness as well as enhanced field localization, which results in the smoother current flow, less losses and better impedance matching, which consequently provide higher efficiency for these antennas — hence they can be applicable for broadband and 5G communications.

4.4 .Comparison with Literature

The designed antennas exhibit better performance than those reported in the literature, with wide multiband operation (4.04–7.73 GHz), and good bandwidths up to 180 MHz, high efficiency (>85%), gain >6 dBi and impedance near 50 Ω within a compact FR-4 substrate (44.5 × 54.25 mm²). Previous designs either used a larger size to achieve wider bandwidth or high gain as [14, 4] or expensive substrates such as the Rogers RT5880 for antenna with higher Gain and efficiency [20,] while some FR-4 antennas had limited multiband operation as well as narrow bandwidths [3, 15]. Slot-loading and metallic nanofilm coatings on FR-4 greatly improve antenna properties, according to recent research: Ag-Au-Ag multilayer coatings boosted bandwidth by ≈18.75% and gain by ≈2 dB, whereas Au nanoparticle coated slots improved bandwidth by ≈12.5% and gain by ≈0.5 dB, allowing for dependable multiband operation without extending the antenna[30].. These improvements reveal the performance gains are accomplished by combining novel design and practical fabrication process, which well explain its higher efficiency, wider bandwidth and multiband features in contrast to the published works.

5. Conclusion

In this study, slotless and slotted ring microstrip patch antennas were designed on FR-4 substrate, fabricated and improved by Nd:YAG laser treatment. Results demonstrate that the slotless antenna changes from dual-band to multi-band, obtaining five resonances from 3.89 to 7.64 GHz, whereas the slotted configuration achieves five resonances between 4.04 and 7.73 GHz with better performance in general. The slot loading and laser polishing result in much better matching impedance, bandwidth, and radiation properties. In particular, the slotted antenna demonstrates a good performance at 5.15 GHz (S11 = –21.7 dB, VSWR = 1.18, BW = 180 MHz) and multiple higher frequency modes are also supported. These results verify that the designed antennas are well-matched to Wi-Fi, Bluetooth, WLAN as well as future 5G systems. For the future, it will be interesting to explore the microstrip circular antenna optimization from AI-based methods, introduce a reconfigurable feature like PIN diodes or varactors inside the design and expand this approach to MIMO/array designs on different substrates or laser parameters.

Acknowledgment

We send our sincere appreciation to all the workers of the Electro-Optics Laboratory in the Physics Department, College of Science, University of Baghdad

Conflict of Interest

The authors declare that they have no conflicts of interest.

Funding

No funding.

References

1. Gopinath D, Marichamy P. On the design and analysis of multi-band micro-strip patch antenna for wireless body area network applications. EURASIP Journal on Wireless Communications and Networking. 2025;2025:24. https://jwcn-eurasipjournals.springeropen.com/articles/10.1186/s13638-025-02442-3
2. Rahayu Yenny, Hidayat Muhammad I. Design of 28/38 GHz dual-band triangular-shaped slot microstrip antenna array for 5G applications. 2018 2nd Int Conf Telematics Future Gener Netw (TAFGEN). IEEE; 2018. p. 93-97. https://ieeexplore.ieee.org/document/8580487
3. Priyalatha P, Kumari R, Nandi S. Compact modified hourglass-shaped aperture-coupled antenna for radar applications. Int J Microw Wirel Technol. 2023;15:1592-1600
4. Taha Bassam, AlSharabati Tareq. Performance comparison between the FR4 substrate and the Rogers Kappa-438 substrate for microstrip patch antennas. Int J Comput Sci Mob Comput. 2020;9:1-12. https://www.academia.edu/download/62010404/V9I2202001202002O6-62010-1wdvj22.pdf
5. Srivastava Ketan, Mishra Bharat, Patel Amit K, Singh Ramesh. Circularly polarized defected ground stub-matched triple-band microstrip antenna for C and X-band applications. Microw Opt Technol Lett. 2020;62:3301-3309. https://onlinelibrary.wiley.com/doi/abs/10.1002/mop.32450
6. Balster J, Pünt I, Stamatialis D F, Wessling M. Multi-layer spacer geometries with improved mass transport. J Memb Sci. 2006;282:351-361. https://www.sciencedirect.com/science/article/pii/S0376738806003711
7. Farha K A, Jasmine P M. Microstrip patch antenna for UWB applications. AIP Conf Proc. 2023;2773:050002. https://pubs.aip.org/aip/acp/article/2773/1/050002/2892505
8. Khidhir Ahmed H. Switching dynamics in terms of effective time constant to determine switching points using a Debye relaxation equation. Iraqi J Sci. 2019: 129–134. https://ijs.uobaghdad.edu.iq/index.php/eijs/article/view/835
9. Abdulzahra D H, Alnahwi F, Abdullah A S, Al-Yasir Y I A, Abd-Alhameed R A. A miniaturized triple-band antenna based on square split ring for IoT applications. Electron. 2022;11:2818. https://www.mdpi.com/2079-9292/11/18/2818

10. Lukacs P, Pietrikova A, Vehec I, Provazek P. Influence of various technologies on the quality of ultra-wideband antenna on a polymeric substrate. Polymers (Basel). 2022;14:507. https://www.academia.edu/download/82676487/pdf.pdf
11. Applications K band, Zahid M, Taqdeer M M, Amin Y. A compact dual-band microstrip patch antenna for C- and X-. 2023;4-9. https://www.mdpi.com/2673-4591/46/1/16
12. Hammas H A, Hasan M F, Jalal A S A. Compact multiband microstrip printed slot antenna design for wireless communication applications. Adv Electromagn. 2020;9:52-59. http://www.aemjournal.org/index.php/AEM/article/view/1393
13. Farghaly S I, Abo Al-Ela K E, Zaki A Y, Fouda H S. New design of microstrip patch antenna at 28 GHZ and 4×4 MIMO configuration with improved characteristics for IoT applications. Eurasip J Wirel Commun Netw. 2025;2025:1. https://link.springer.com/article/10.1186/s13638-025-02486-5
14. Pallavi H V, Chandra A P J. Design of slotted circular microstrip patch antenna array for 5G millimeter-wave applications. 2021. https://www.researchgate.net/publication/355978263_Design_of_Slotted_Circular_Microstrip_Patch_Antenna_Array_for_5G_Millimeter-Wave_Applications
15. Prashanth K, Jayakrishna Sai C, Srihari B L, Manisha K. Design of micro-strip patch antenna for C-band applications. E3S Web Conf. 2023;391:1-8. https://www.e3s-conferences.org/articles/e3sconf/abs/2023/28/e3sconf_icmed-icmpc2023_01066/e3sconf_icmed-icmpc2023_01066.html
16. Naik M N. Design of compact annular ring microstrip antenna for multiband communication system. J Netw Commun Emerg Technol. 2017;7:24-28. https://www.jncet.org/Manuscripts/Volume-7/Issue-8/Vol-7-issue-8-M-05.pdf
17. Textile B, Ring R, Patch M. At 2.45 GHz for wearable applications. 2021;1-17. https://ieeexplore.ieee.org/document/9739680
18. Moura C G, Dinis H, Carvalho O, Mendes P M, Nascimento R M, Silva F S. A novel approach for micro-antenna fabrication on ZrO2 substrate assisted by laser printing for smart implants. Appl Sci. 2022;12:9333. https://www.mdpi.com/2076-3417/12/18/9333
19. Huang S, Zeng J, Wang W, Zhao Z. Study on laser polishing of Ti6Al4V fabricated by selective laser melting. Micromachines. 2024;15:336. https://www.mdpi.com/2072-666X/15/3/336
20. Kareem Q H, Abdullah L W, Shihab R A, Al-Hasani F A J, Abdullah S N. Optimize the performance of reconfigurable antenna based on laser treatment for sub-6GHz applications. Prog Electromagn Res Lett. 2025;123.
21. Ahmed Fayyadh H. Frequency reconfigurable monopole antenna using switchable slotted triangular radiators. Eng Technol J. 2018;36(2). https://iasj.rdd.edu.iq/journals/uploads/2025/01/09/2bd7e0565c4a2ba879807192eb1b8699.pdf
22. Bahaa B, Elias Q, Bashar B S, Alanssari A I, Soh P J, Misran H. A metasurface-based high-gain patch antenna for future multiband wireless communication. 2024;7:47-60. https://doi.org/10.31987/ijict.7.1.268
23. Habib N F, Wadday A G, Ali F M. Design multiband compact microstrip circular slot fractal meta-surface antenna. 2024;1–11 [PDF]. https://iasj.rdd.edu.iq/journals/uploads/2024/12/06/28b3e6d1cf2b648f7c65cb32ef515e15.pdf
24. Mustafa F I, Shakir S, Mustafa F F, Naiyf A T. Simple design and implementation of solar tracking system two axis with four sensors for Baghdad city. 2018 9th Int Renew Energy Congr (IREC). IEEE; 2018. p. 1-5. https://ieeexplore.ieee.org/document/8355789
25. Kadpan W R, Mustafa F F, Kadhim H T. A review of control automatically water irrigation canal using multi controllers and sensors. J Eur des Syst Autom. 2024;57:717-727. https://doi.org/10.18280/jesa.570309
26. Ahmed S, Albehadili A A, Mohammed Z H, Hassain Z A, Al-saadi M, Chandra M. Circularly polarized hexagonal microstrip antenna loaded with slot and complementary split ring resonator. 2024;28:06.: https://doi.org/10.31272/jeasd.28.6.7
27. Alblaihed K A, Abbasi Q H, Imran M A, Mohjazi L. Wideband of microstrip patch antenna for 28 GHz 5G applications. 2023;189-190.https://eprints.gla.ac.uk/294715/1/294715.pdf
28. Souryendu Das, Gokhroo S. Microstrip Patch Antenna at 7 GHz for Satellite Communication. IJETSR. 2015;2(11):1-11. https://ssrn.com/abstract=322900

29. Kashyap PA, Sarmah K, Dakua I, Baruah S. Gain and bandwidth enhancement of slotted microstrip antenna using metallic nanofilms for WLAN applications. Journal of King Saud University – Science. 2023;35(1):102374. https://doi.org/10.1016/j.jksus.2022.102374
30. Khidhir A H. Effect of surface recombination on diffusion length and active cavity life time. Iraqi J Sci. 2020;3215-3220. https://ijs.uobaghdad.edu.iq/index.php/eijs/article/view/2003